AD-A045 144 GRUMMAN AEROSPACE CORP BETHPAGE N Y RESEARCH DEPT F/G 14/5
THE FORMATION AND OPTIMIZATION OF INTERFEROMETRIC FRINGES.(U)
SEP 77 B J PERNICK, K G LEIB

UNCLASSIFIED RM-642 NL

1 OF 1
AD
A045144

END
DATE FILMED
11-77
DDC

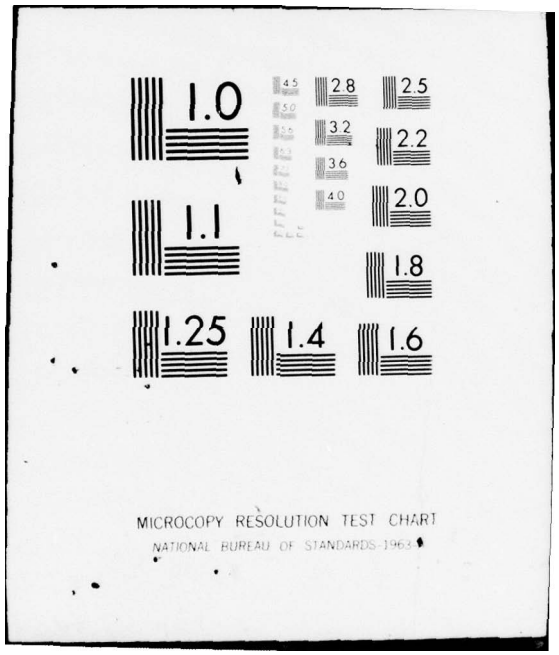
1.0
1.1
1.25
1.4
1.6
1.8
2.0
2.2
2.5
2.8
3.2
3.6
4.0
4.5
5.0
MICROCOPY RESOLUTION TEST CHART
NATIONAL BUREAU OF STANDARDS-1963-A

(12)

RM-642

THE FORMATION AND OPTIMIZATION OF INTERFEROMETRIC FRINGES

September 1977

RESEARCH DEPARTMENT

GRUMMAN AEROSPACE CORPORATION
BETHPAGE, NEW YORK

UNCLASSIFIED

SECURITY CLASSIFICATION OF THIS PAGE *(When Data Entered)*

REPORT DOCUMENTATION PAGE		READ INSTRUCTIONS BEFORE COMPLETING FORM
1. REPORT NUMBER RM-642	2. GOVT ACCESSION NO.	3. RECIPIENT'S CATALOG NUMBER
4. TITLE *(and Subtitle)* The Formation and Optimization of Interferometric Fringes		5. TYPE OF REPORT & PERIOD COVERED
		6. PERFORMING ORG. REPORT NUMBER RM-642
7. AUTHOR(s) Benjamin J. Pernick and Kenneth G. Leib		8. CONTRACT OR GRANT NUMBER(s)
9. PERFORMING ORGANIZATION NAME AND ADDRESS Research Department Grumman Aerospace Corporation Bethpage, New York 11714		10. PROGRAM ELEMENT, PROJECT, TASK AREA & WORK UNIT NUMBERS
11. CONTROLLING OFFICE NAME AND ADDRESS		12. REPORT DATE September 1977
		13. NUMBER OF PAGES
14. MONITORING AGENCY NAME & ADDRESS*(if different from Controlling Office)*		15. SECURITY CLASS. *(of this report)* Unclassified
		15a. DECLASSIFICATION/DOWNGRADING SCHEDULE

16. DISTRIBUTION STATEMENT *(of this Report)*

Approved for Public Release; Distribution Unlimited

17. DISTRIBUTION STATEMENT *(of the abstract entered in Block 20, if different from Report)*

18. SUPPLEMENTARY NOTES

19. KEY WORDS *(Continue on reverse side if necessary and identify by block number)*

Matched Filters or Holographic Lenses

20. ABSTRACT *(Continue on reverse side if necessary and identify by block number)*

Expressions to describe fringe contours in the region of interference of two coherent beams are derived for three combinations of plane and spherical wave geometries. The fringe contrast ratio is shown to be spatially variable whenever spherical wavefronts are involved and can be controlled by altering the reference to signal beam intensity ratio. These expressions can be applied during the fabrication of matched filters or holographic lenses.

DD FORM 1 JAN 73 1473 EDITION OF 1 NOV 65 IS OBSOLETE
S/N 0102-014-6601

UNCLASSIFIED
SECURITY CLASSIFICATION OF THIS PAGE *(When Data Entered)*

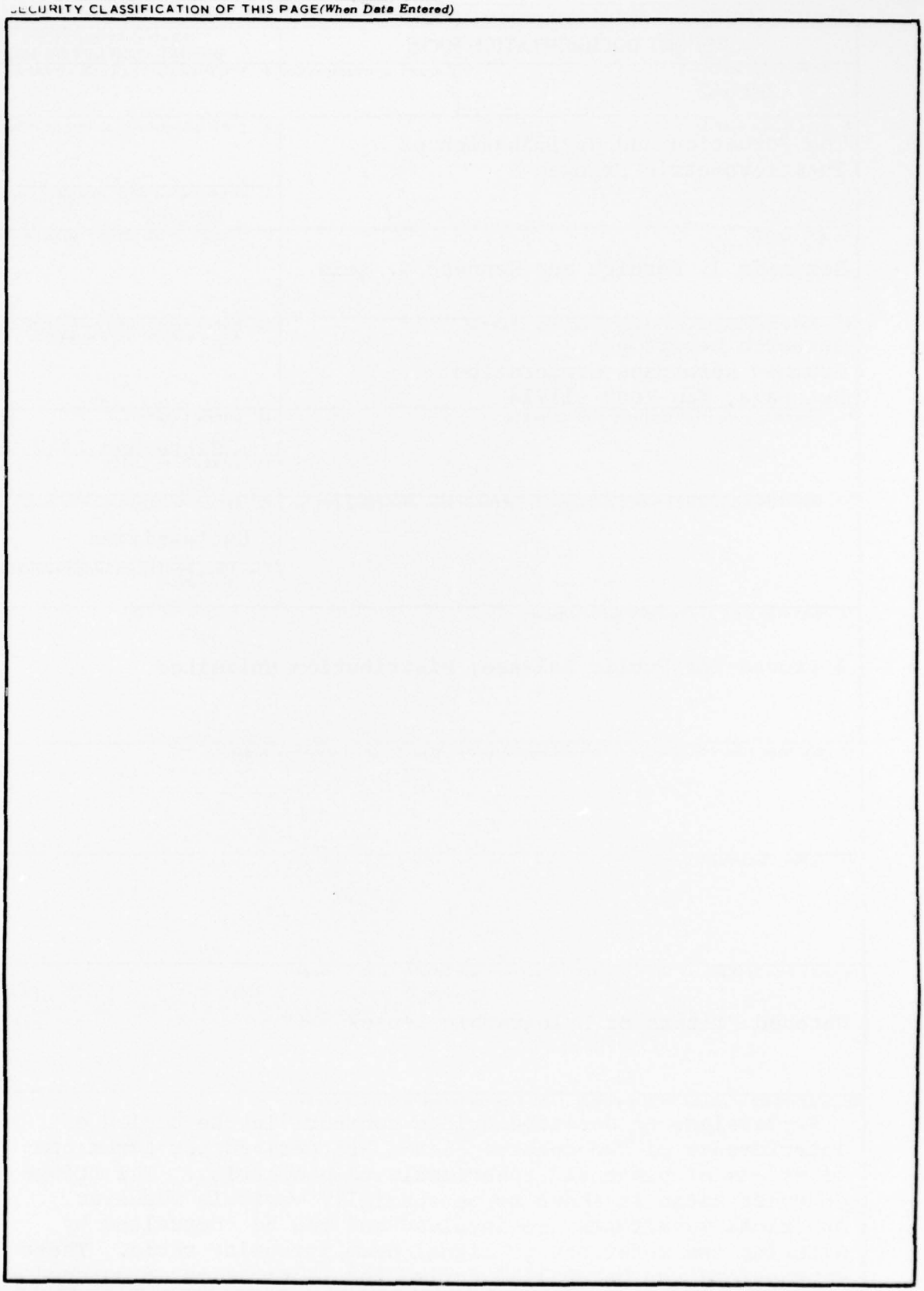

(9) (14)

Grumman Research Department Memorandum RM-642

rept.

(6)

THE FORMATION AND OPTIMIZATION OF INTERFEROMETRIC FRINGES

by

(10) Benjamin J. Pernick

and

Kenneth G. Leib

System Sciences

(11) September 1977

(12) 37 p.

Approved by: Richard A. Scheuing
Richard A. Scheuing
Director of Research

ABSTRACT

Expressions to describe fringe contours in the region of interference of two coherent beams are derived for three combinations of plane and spherical wave geometries. The fringe contrast ratio is shown to be spatially variable whenever spherical wavefronts are involved and can be controlled by altering the reference to signal beam intensity ratio. These expressions can be applied during the fabrication of matched filters or holographic lenses.

INTRODUCTION

Interference fringe patterns are the means with which optical wavefront information is recorded and stored in applications of holography, matched filtering, and in optical component testing with interferometric techniques. Consequently, an understanding of fringe pattern properties obtained with several rudimentary geometric systems is of practical value in devising test techniques, as well as in fostering an understanding of more complicated geometries. These are of more than academic interest; the setups are used in such applications as beam collimation checks and holographic lens preparation. Fringe characteristics are influenced by several factors: relative intensities of the signal and reference beams; orientations; wavelength; coherence; state of polarization; and beam motion or environment-induced optical path length changes. We are concerned primarily with the first two significant factors in this note. Other items, namely the influence of coherence on fringe visibility (Refs. 1 and 2) the effects of intentional motion or path length

changes (Ref. 3), and methods to alleviate the adverse effects of unwanted motion and techniques to stabilize fringe recording systems (Ref. 4) have been discussed in the literature as noted. Wavelength is assumed to be constant. Also, the influence of the photographic recording technique is not considered.

The intent of this note is to determine the interference fringe pattern characteristics that are obtained with combined plane wave and spherical wave geometries. Three fundamental arrangements are considered: the interference of two plane waves, of a plane and a spherical wave, and of two spherical waves. In all three cases we find an equation for the light intensity distribution in a plane in the region of beam overlap, determine contours of intensity maxima and minima in this plane (i.e., fringe geometry), and contrast ratios. The contrast ratio is shown to be variable across the interference or recording plane whenever a spherical wave is used, and can be easily optimized.

BASIC NOTATION

Figure 1 shows a signal beam and a reference beam incident upon the planar surface of a holographic recording or interferometer observation plane located in the region of interference. The origin of a coordinate system is located in this plane and is oriented for convenience so that the x,z-plane is in the plane of incidence, as illustrated. The y-axis is directed normal to the plane of the figure. The z-axis is also called the optic axis. The angles of incidence for reference and signal beams are labeled ψ_R and ψ_S, respectively. For our purposes, these angles of incidence are measured with respect to a direction parallel to the optic or z-axis. Note that the incident angle is constant for each ray of light in a collimated beam with planar wavefronts. On the other hand, the incident angle for each light ray in a spherically diverging beam (or in general, a nonplanar wavefront) varies with each ray path. This ray path variation coupled with an arbitrary placement of a recording plane account for the wide variations in fringe characteristics.

It is conventional to describe the amplitude of an optical signal in exponential form explicitly omitting the exponential time factor, $\exp(j\omega t)$. This can be done since the time factor is common to both light beams (i.e., the beams are temporally coherent). The spatial dependence of the reference beam amplitude is written as

$$\begin{aligned} R(x,y,z) &= R_o \exp(jk\bar{s}_r \cdot \bar{r}) \\ &= R_o \exp[jk(p_r x + q_r y + m_r z)] \end{aligned} \tag{1}$$

Here, R_o represents the magnitude of the complex reference beam amplitude, $k = 2\pi/\lambda$ where λ is the wavelength, $\bar{s}_r$ is a unit vector in the direction of propagation of the reference beam, and $\bar{r}$ is a position vector to the point at which the reference beam amplitude function is measured. The direction cosines of the unit vector $\bar{s}_r$ are p_r, q_r, and m_r, and the components of the position vector $\bar{r}$ are x, y, and z. Note that the reference beam intensity is given by $[R(x,y,z) \cdot R^*(x,y,z)] = R_o^2$ where the $*$ denotes complex conjugate. If the reference beam is a plane wave then R_o is a constant independent of position [otherwise one has, in general, $R_o = R_o(x,y,z)$]. Quantities in the exponent of Eq. (1) determine the phase in terms

of the components of $\bar{s}_r$ and $\bar{r}$. The unit vector $\bar{s}_r$ is constant for a plane wave and spatially variable for other wavefronts.

If the reference beam is a plane wave we shall denote its amplitude by Eq. (1). However, for a reference beam with spherical wavefront, we use the expression

$$R(x,y,z) = (\text{const}/\rho)\exp(jk\rho) \qquad (2)$$

where ρ represents the distance from a point source (origin of the spherical wavefront) to any given point in space. Since the unit propagation vector in this case is a radial vector, the phase term is $k\rho$; i.e., surfaces of constant phase are spheres for which ρ = const.

The signal beam is either a plane or spherical wave and therefore expressed by

$$S(x,y,z) = S_o \exp(jk\bar{s} \cdot \bar{r} + j\Phi) \qquad (3)$$

or

$$S(x,y,z) = (\text{const}/\rho)\exp(jk\rho + j\Phi) \qquad (4)$$

in analogy with Eqs. (1) and (2). The unit vector in the direction of propagation is now labeled $\bar{s}$. For generality, the quantity Φ represents a constant phase difference between both beams (i.e., the refer-

ence and signal beams are usually derived from a common source).

In the region of beam overlap the resultant beam amplitude is just the sum

$$A(x,y,z) = R(x,y,z) + S(x,y,z) \tag{5}$$

and the corresponding light intensity at points in the three dimensional region of interference is given by

$$\begin{aligned} I(x,y,z) &= A(x,y,z) \cdot A^*(x,y,z) \\ &= RR^* + SS^* + RS^* + SR^* \end{aligned} \tag{6}$$

INTERFERENCE OF TWO PLANE WAVES

Figure 2 illustrates the overlap and interference of two plane waves. Let the direction cosines of the unit vector $\bar{s}$ for the plane wave signal beam be written as p, q, and m. Then, from Eq. (3) one has

$$S(x,y,z) = S_o \exp[jk(px + qy + mz) + j\phi] \tag{7}$$

In the region of beam overlap, the light intensity distribution in the interference pattern is obtained from Eqs. (1), (6), and (7). One has

$$I(x,y,z) = R_o^2 + S_o^2 + 2R_oS_o \cos [k\bar{r} \cdot (\bar{s} - \bar{s}_r) + \phi] \tag{8}$$

where

$$\bar{r} \cdot (s - s_r) = (p - p_r)x + (q - q_r)y + (m - m_r)z \qquad (9)$$

Note that the intensity pattern of Eq. (8) is constant for regions in space where the argument of the cosine function is constant, i.e., along planes in space described by the equation

$$\bar{r} \cdot (\bar{s} - \bar{s}_r) = \text{constant} \qquad (9a)$$

Since both propagation vectors $\bar{s}$ and $\bar{s}_r$ lie in the plane of incidence, then $q = 0 = q_r$. Furthermore, in the observation or holographic recording plane one has $z = 0$. Thus the intensity distribution in this plane becomes, using Eqs. (8) and (9)

$$I(x,y,0) = R_o^2 + S_o^2 + 2R_oS_o \cos[k(p - p_r)x + \Phi] \qquad (10)$$

This well known intensity profile is illustrated in Fig. 3. The intensity curve is periodic in terms of the x-variable. Clearly the maxima and minima values for $I(x,y,0)$ occur at x-values for which the cosine term is ± 1, respectively, i.e., the argument of the cosine term is an even or odd multiple of π. Specifically, intensity maxima occur when

$$k(p - p_r)x_{max} + \Phi = 2n\pi \quad , \quad n = 0, \pm 1, \pm 2, \ldots \qquad (11)$$

and intensity minima when

$$k(p - p_r)x_{min} + \phi = (2n + 1)\pi \qquad (12)$$

The interference fringe lines (corresponding to equal intensity contours) appear as a family of straight lines parallel to the y-axis.

The fringe line spacing or spatial period is from either Eq. (11) or Eq. (12)

$$\Delta x = \lambda/(p - p_r) \qquad (13)$$

For example, if the reference beam propagation is in the z-direction, then $\psi_r = 0$, and consequently $p_r = \sin \psi_r = 0$. Thus $p = \sin \psi_s$ and

$$\Delta x = \lambda/\sin \psi_s \qquad (14)$$

If both reference and signal beams are symmetrically oriented about the z-axis, then $p_r = -p = -\sin \psi_s$ and the fringe spacing is obtained from

$$\Delta x = \lambda/2 \sin \psi_s \qquad (15)$$

Finally, for any arbitrary pair of beam orientations in the plane of incidence, the fringe separation follows from Eq. (13)

$$\Delta x = \lambda/(\sin \psi_s \pm \sin \psi_r) \qquad (16)$$

The positive sign is used when the reference beam incident angle is oriented opposite to the signal beam angle

(as shown in Fig. 2); the negative sign is used when both incident angles are oriented in the same angular direction from the optic axis. Fringe separations depicting Eqs. (14) and (15) are summarized in Fig. 4. It is of interest to note that for certain cases fringe spacings for the asymmetrical case described by Eq. (16) are those values which are bounded by the two illustrated curves (e.g., if the angles are oppositely oriented and $\psi_r < \psi_s$).

The contrast ratio is a "figure of merit" of the fringe pattern that describes the depth of modulation for the sinusoidal fringe pattern previously illustrated in Fig. 3. The contrast ratio is defined as*

$$C_R = \frac{I_{max} - I_{min}}{I_{max} + I_{min}} \tag{17}$$

where I_{max} refers to the maximum intensity value in the interference pattern and is given by $(R_o + S_o)^2$.

---

*Other definitions use $C_R = I_{max}/I_{min}$ as the contrast ratio for images and, hence, the photographic result of recording the fringes. Also $(I_{max} - I_{min})$ is often called the depth of modulation.

Thus, the contrast ratio can be written as

$$C_R = \frac{(R_o + S_o)^2 - (R_o - S_o)^2}{(R_o + S_o)^2 + (R_o - S_o)^2} \tag{18}$$

Defining the beam ratio as

$$R = \frac{\text{Reference Beam Intensity}}{\text{Signal Beam Intensity}} \equiv \frac{R_o^2}{S_o^2}$$

we obtain

$$C_R = \frac{2\sqrt{R}}{1 + R} \tag{19}$$

A plot of the contrast ratio as a function of the beam ratio given by Eq. (19) is shown in Fig. 5, as the curve marked $\theta = 0$. C_R has a maximum value of unity at $R = 1$, and for the case of two interfering plane waves, is constant across a recording plane.

As a practical illustration, the shearing interferometric method for establishing a collimated beam involves the interference of two plane waves. The shearing interferometer consists of a slightly wedged optical flat mounted so that the plane of the wedge angle is perpendicular to the plane of the mounting base (see Fig. 6). A straight wire is often mounted across the face of the flat and set parallel to the

base plane as a fringe reference.*

The collimated beam condition is illustrated in Fig. 6. The collimated beam is divided into two beams, one as a reflection from the front surface, the other a rear surface reflection. Both reflected beams travel at a slight angle and form interference fringes. These fringes will be parallel to the reference wire (and themselves) when the incident beam is collimated. Alternately, the ability to form a straight line fringe field is useful as a visual check on the "quality" of the collimation. One could also use this interference fringe pattern in another way, i.e., to determine the wedge angle, assuming the incident beam to be collimated.

INTERFERENCE OF A PLANE AND SPHERICAL WAVE

The optical setup to achieve the interference of a plane and spherical wave is shown in Fig. 7. For generality, we locate the point source of the spherical wave at the position (a,b,c) with respect to an arbitrarily chosen coordinate origin. Two cases of interest

*A shearing interferometer is manufactured by the Continental Optical Corporation, Hauppauge, New York 11787.

to be discussed are characterized by placing the point source of light of the spherical wave on the system optic or z-axis, or alternately placing the point source off the z-axis. The angular orientation of the plane wave is arbitrary.

The distance from the point source to any other point in space is given by

$$p = \sqrt{(x - a)^2 + (y - b)^2 + (z - c)^2} \qquad (20)$$

The beam amplitudes, given by Eqs. (1) and (4), are summed and the net beam intensity in the three dimensional region of overlap is found to be

$$I(x,y,z) = R_o^2 + S^2/\rho^2 + (2SR_o/\rho)\cos\left\{k(\rho - \bar{s}_r \cdot \bar{r}) + \phi\right\} \qquad (21)$$

(Note that the reference beam phase is assumed to be zero at the arbitrary origin.)

The conditions for maximum and minimum intensity values are again obtained by setting the argument of the cosine function equal to an even or odd multiple of π, respectively. Thus, for a maximum resultant intensity one requires that

$$k(\rho - \bar{s}_r \cdot \bar{r}) + \Phi = 2n\pi \quad , \quad n = 0, \pm 1, \pm 2, \ldots \tag{22}$$

and for a minimum one requires

$$k(\rho - \bar{s}_r \cdot \bar{r}) + \Phi = (2n + 1)\pi \quad , \quad n = 0, \pm 1, \pm 2, \ldots \tag{23}$$

To demonstrate the geometrical properties of the interference fringe patterns described by Eqs. (22) and (23) we introduce the quantity

$$\alpha_n = \rho - \bar{s}_r \cdot \bar{r} \tag{24}$$

where $\alpha_n = (2n\pi - \Phi)/k$ or $[(2n + 1)\pi - \Phi]/k$ from Eqs. (22) and (23), respectively. In terms of the direction cosines for the plane wave, one has

$$\rho = p_r x + q_r y + m_r z + \alpha_n \tag{25}$$

Squaring both sides of Eq. (25) and combining with Eq. (20) leads to

$$\begin{aligned} &(1 - p_r^2)x^2 + (1 - q_r^2)y^2 + (1 - m_r^2)z^2 \\ &- 2(a + p_r\alpha_n)x - 2(b + q_r\alpha_n)y - 2(c + m_r\alpha_n)z \\ &- 2p_r q_r xy - 2q_r m_r yz - 2p_r m_r xz \\ &= \alpha_n^2 - (a^2 + b^2 + c^2) \end{aligned} \tag{26}$$

This result is in the form of an equation for a family of ellipsoidal surfaces in space. These surfaces are equiphase surfaces for the maximum or minimum intensities as the case may be, but the intensity pattern is not necessarily uniform on a given ellipsoidal surface because of the factors $1/\rho$, $1/\rho^2$ in the intensity, see Eq. (21). Consequently the intensity does, in general, depend upon the radial distance ρ. It is clear then that the surfaces of equal visibility are nonplanar (as was the case with two interfering plane waves).

Let an observation (or recording) plane be described by the linear equation

$$Ax + By + Cz = D \tag{27}$$

In this plane, the interference fringes form a series of elliptical shapes. This can be demonstrated by solving Eq. (27) for the quantity z and substituting the result into Eq. (26), i.e., finding the intersection of an ellipsoid and a plane. The resultant equation is quadratic in x and y and is of the form of a family of ellipse contours in the observation plane. As noted above there will be a variation in fringe visibility in this plane.

Two specific cases are of practical interest. First assume that the reference beam is oriented such that the direction cosine $q_r = 0$ and that $z = 0$ in the observation plane. Equation (26) then reduces to

$$(1 - p_r^2)x^2 + y^2 - 2(a + p_r\alpha_n)x - 2by = \alpha_n^2 - (a^2 + b^2 + c^2) \tag{28}$$

which is representative of a family of ellipses in this specific observation plane. Since $1 - p_r^2 \leq 1$ the semimajor axis is oriented parallel to the x-axis. Once again the fringe spacing is not constant over the plane of interference.

As a second example, assume that the reference beam is directed along the z-axis. For this special orientation the direction cosine $p_r = 0$ as well. Thus, Eq. (28) reduces to

$$x^2 + y^2 - 2ax - 2by = \alpha_n^2 - (a^2 + b^2 + c^2)$$

or

$$(x - a)^2 + (y - b)^2 = \alpha_n^2 - c^2 \tag{29}$$

The interference fringe pattern consists of a family of concentric circles in the observation plane that are centered about the point (a, b). For convenience one

can take $a = 0 = b$ to simplify the above results.

We can readily estimate the fringe spacing for this case. For example, intensity maxima are located at positions where $k\rho_{max} = 2n\pi - \varphi$, from Eq. (22). The change in ρ for consecutive n-values is

$$\Delta\rho = \frac{1}{k}\left[\left(2(n+1)\pi - \phi\right) - (2n\pi - \phi)\right] = \frac{2\pi}{k} = \lambda \quad (30)$$

If $r = \sqrt{x^2 + y^2}$ is the polar coordinate in the observation plane where $z = 0$ then, from Eq. (20)

$$\rho^2 = x^2 + y^2 + c^2 = r^2 + c^2 \quad (31)$$

The fringe separation in the observation plane is approximated by

$$\Delta r \simeq \rho\Delta\rho/r = \sqrt{1 + c^2/r^2}\ \Delta\rho = \sqrt{1 + c^2/r^2}\ \lambda \quad (32)$$

The fringes appear as a family of circular rings, however the fringe spacing Δr is not constant; rather it decreases for increasing r-values as indicated by Eq. (32).

The (relative) maximum value of the light intensity in the plane of observation is from Eqs. (21) and (22)

$$I_{max} = R_o^2 + S^2/\rho_{max}^2 + 2SR_o/\rho_{max} = (R_o + S^2/\rho_{max})^2 \quad (33)$$

The (relative) minimum value is from Eqs. (21) and (23)

$$I_{min} = R_o^2 + S^2/\rho_{min}^2 - 2SR_o/\rho_{min} = (R_o - S/\rho_{min})^2 \quad (34)$$

Thus the contrast ratio, defined by Eq. (17), can be written as

$$C_R = \frac{(R_o + S/\rho_{max})^2 - (R_o - S/\rho_{min})^2}{(R_o + S/\rho_{max})^2 + (R_o - S/\rho_{min})^2} \quad (35)$$

For regions of the interference fringe pattern where the fringe spacing is small compared to the distance to the source, one can approximate

$$\rho_{max} \simeq \rho_{min} \simeq c/\cos\theta \quad (36)$$

where θ is the angle between the optic axis and the line segment joining the point source and a typical observation point in the vicinity of ρ_{max} or ρ_{min}. With this approximation the contrast ratio can be written as

$$C_R = \frac{2\sqrt{\mathcal{R}}\cos\theta}{\mathcal{R} + \cos^2\theta} \quad (37)$$

where the beam ratio $\mathcal{R}$ is now defined as

$$\mathcal{R} = \left\{\frac{CR_o}{S}\right\}^2 \quad (38)$$

Equation (37) demonstrates that with this plane wave-spherical wave geometry the contrast visibility varies across the observation plane.

The plot of contrast ratio as a function of the signal/reference beam ratio, previously illustrated in Fig. 5 for the case of two interfering plane waves, can be used to portray the contrast ratio function of Eq. (37). Define the "modified" beam ratio as

$$R' = R/\cos^2 \theta \tag{39}$$

In terms of R', Eq. (37) becomes

$$C_R = \frac{2\sqrt{R'}}{1 + R'} \tag{40}$$

which is of the same functional form as Eq. (19). Thus Fig. 5 represents C_R in a condensed form as a function of R'. The maximum contrast ratio $C_R = 1$ only for points in the observation plane where $R' = R/\cos^2 \theta = 1$ or equivalently, where $\cos^2\theta = R$. This is an important result. It means that maximum contrast is obtained with a beam ratio less than one; quite different than the requirement with two plane waves. The contrast ratio curve is also illustrated for a particular value of $\theta = 60°$.

As a second practical example, consider the fabrication of a high spatial frequency optical matched filter to improve the signal-to-noise ratio. Since the contrast ratio is not constant, points near the center of the pattern have higher contrast ratios than those of more remote points at

higher spatial frequency values. One can envision compensation for this contrast fall-off in the filter plane to enhance favorably the higher spatial frequency signals (note that the fall-off in response of film at higher spatial frequencies further degrades contrast).

INTERFERENCE OF TWO SPHERICAL WAVES

This beam configuration is illustrated in Fig. 8. The point sources are located at distances d_1 and d_2 from the observation plane. The plane of incidence is determined by these two point sources and the z or optic axis. A coordinate system is centered between the two point sources as indicated in the figure.

Let ρ_1 and ρ_2 represent the distances from each point source to a position in the region of interference. Then

$$\rho_1 = \sqrt{(x - a)^2 + y^2 + (z + d_1)^2}$$
$$\rho_2 = \sqrt{(x + a)^2 + y^2 + (z + d_2)^2} \qquad (41)$$

Beam amplitudes in the observation plane are given by

$$S_1(x,y,o) = \frac{S_1}{\rho_1} e^{jk\rho_1}$$

$$S_2(x,y,o) = \frac{S_2}{\rho_2} e^{j(k\rho_2 + \phi)} \tag{42}$$

where S_1, S_2, and ϕ are constants. Consequently, the intensity profile of the combined beams reduces to

$$I = \frac{S_1^2}{\rho_1^2} + \frac{S_2^2}{\rho_2^2} + \frac{2S_1S_2}{\rho_1\rho_2} \cos\left\{k(\rho_2 - \rho_1) + \phi\right\} \tag{43}$$

The conditions for local extremum values of the intensity distribution are given by

$$k(\rho_2 - \rho_1) + \phi = 2n\pi \tag{44}$$

for a maximum and

$$k(\rho_2 - \rho_1) + \phi = (2n + 1)\pi \tag{45}$$

for a minimum, where $n = 0, \pm1, \pm2, \ldots$. In the region of interference the fringe contours described by Eqs. (44) and (45) are next shown to be quadratic surfaces.

We set $\alpha_n = (2n\pi - \phi)/k$ for a maximum or $\alpha_n = [(2n + 1)\pi - \phi]/k$ for a minimum; thus from either Eqs. (44) or (45)

$$\rho_2 - \rho_1 = \alpha_n \tag{46}$$

or

$$\rho_2^2 - \rho_1^2 = \alpha_n^2 + 2\alpha_n\rho_1 \tag{47}$$

Using Eqs. (41), Eq. (47) reduces at first to

$$4x^2 + [d_2^2 - d_1^2 - \alpha_n^2] + 2(d_2 - d_1)z = 2\alpha_n\rho_1 \tag{48}$$

and finally in terms of the x,y,z coordinates

$$\begin{aligned}(16a^2 - 4\alpha_n^2)x^2 - 4\alpha_n^2y^2 + [4(d_2 - d_1)^2 - 4\alpha_n^2]z^2 \\ + 8a(d_2^2 - d_1^2)x + 4[(d_\alpha - d_1)\beta + 2\alpha_n^2d_1]z \\ + 16a(d_2 - d_1)xz + [\beta^2 - 4\alpha_n^2(a^2 + d_1^2)] = 0\end{aligned} \tag{49}$$

where

$$\beta \equiv d_2^2 - d_1^2 - \alpha_n^2$$

Two interesting cases serve to illustrate the nature of the fring contours. In the plane $z = 0$, Eq. (49) simplifies to

$$\begin{aligned}(16a^2 - 4\alpha_n^2)x^2 - 4\alpha_n^2y^2 \\ + 8a(d_2^2 - d_1^2)x + [\beta^2 - 4\alpha_n^2(a^2 + d_1^2)] = 0\end{aligned} \tag{50}$$

Furthermore, if we consider the arrangement for which $d_1 = d_2$, then one has

$$(16a^2 - 4\alpha_n^2)x^2 - 4\alpha_n^2y^2 + \alpha_n^2[\alpha_n^2 - 4(a^2 - d_1^2)] = 0 \tag{51}$$

If the coefficient of the x^2 term is positive then Eq. (51) represents a family of hyperbolic curves in the recording plane. On the other hand, if this coefficient is negative then Eq. (51) represents a family of hyperbolic or elliptic curves depending upon the sign of the last, constant term in the equation.

As a final example let the two point sources lie on the optic axis. Setting $a = 0$ in Eq. (41) yields

$$\rho_1 = \sqrt{x^2 + y^2 + d_1^2}$$
$$\rho_2 = \sqrt{x^2 + y^2 + d_2^2} \tag{52}$$

Squaring and subtracting results in

$$\rho_2^2 - \rho_1^2 = d_2^2 - d_1^2 \tag{53}$$

where we assume $d_2 > d_1$. From Eq. (47) one has

$$d_2^2 - d_1^2 = \alpha_n^2 + 2\alpha_n \rho 1 \tag{54}$$

or, in terms of the x,y coordinates, Eq. (54) reduces to

$$x^2 + y^2 = \frac{(d_2^2 - d_1^2 - \alpha_n^2)^2}{4\alpha_n^2} - d_1^2 \tag{55}$$

Thus, the interference fringe patterns are circular, with a common center located at the origin of coordinates in the observation plane.

The contrast ratio for this two-spherical beam set-up can be easily determined as

$$C_R = \frac{\left(2 \frac{S_2}{S_1} \frac{\rho_1}{\rho_2}\right)}{1 + \left(\frac{S_2}{S_1} \frac{\rho_1}{\rho_2}\right)^2} \tag{56}$$

or, defining $\mathcal{R} \equiv \left((S_2/S_1)(\rho_1/\rho_2)\right)^2$

$$C_R = \frac{2\sqrt{\mathcal{R}}}{1 + \mathcal{R}} \tag{57}$$

The contrast ratio has the same function form as in Eqs. (19) and (40) and depends upon the spatially variable quantity ρ_1/ρ_2.

CONCLUSIONS

We have derived equations for the interference fringe contour for combinations of plane and spherical waves in the volume of interference. Spherical wavefronts give rise to contrast ratios that are spatially variable which can be a nonoptimum condition in recording patterns. Control of the beam ratio can be effected to provide the desired optimized conditions in holography, matched filter fabrication, or any particular applications.

REFERENCES

1. M. Born and E. Wolf, "Principles of Optics," Pergamon Press, New York, Chapter, 10, 1964.
2. G. B. Parrent, Jr. and B. J. Thompson, "Physical Optics Notebook," Society of Photo-Optical Instrumentation Engineers, California, Chapters, 10, 11, and 12, 1969.
3. C. C. Aleksoff, "Temporally Modulated Holography," Appl. Optics, 10, 1329, 1971.
4. B. J. Pernick and M. Kesselman, "Stabilization of Holographic Recording Systems with Intermittent Exposure Control," Rev. Sci. Instrum., 43, 579, 1972.

FIGURES

Figure

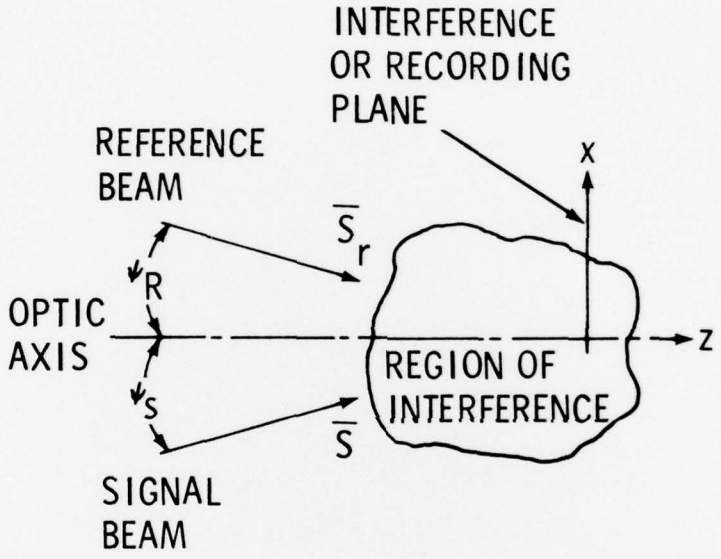

Fig. 1 Coordinate system and general beam geometry

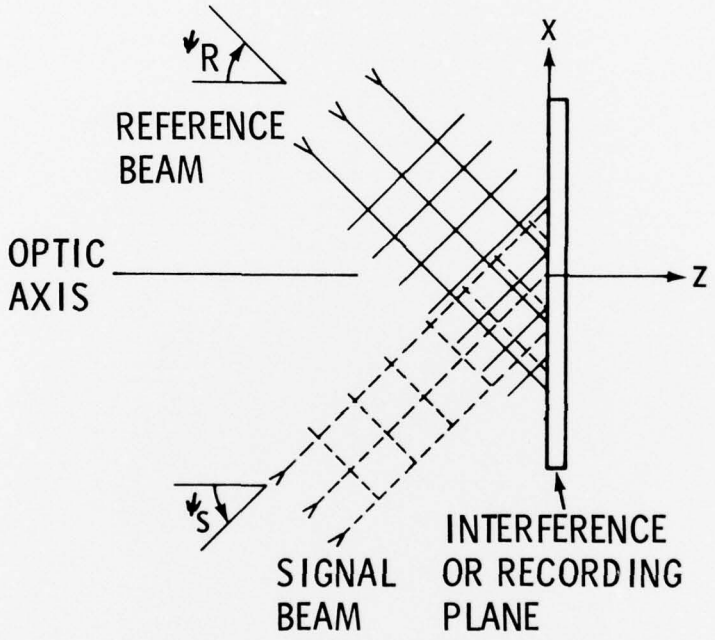

Fig. 2 Interference of two plane waves

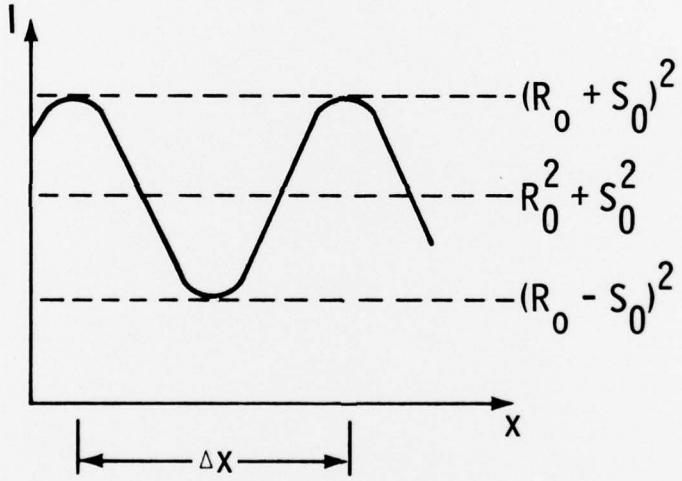

Fig. 3 Intensity profile of interference pattern of two plane waves

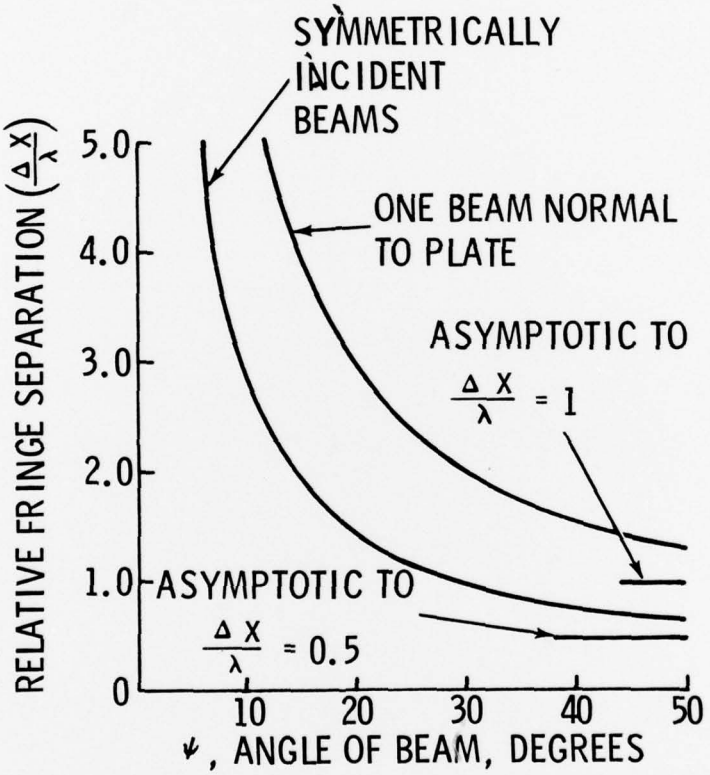

Fig. 4 Fringe separation as a function of plane wave beam orientations

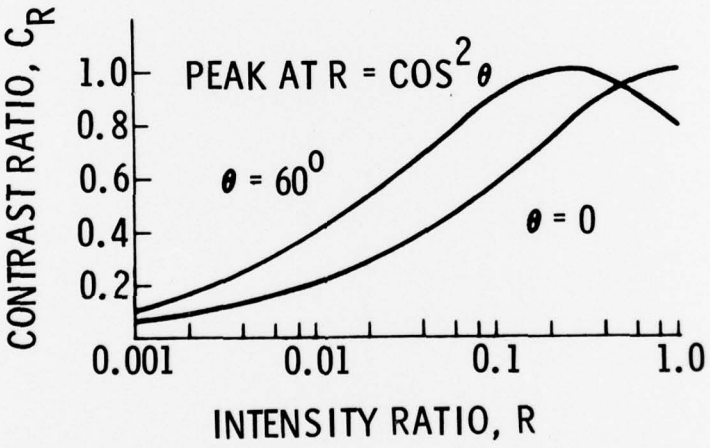

Fig. 5 Contrast ratio as a function of the beam ratio

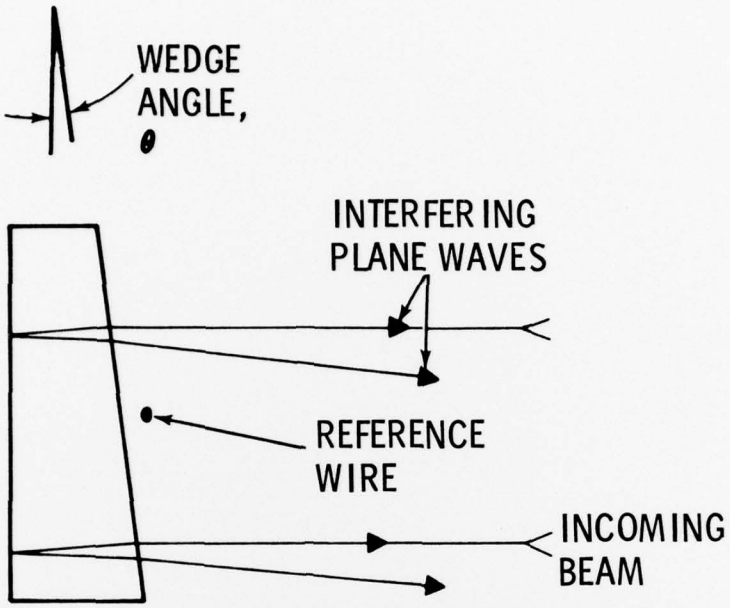

(a) SIDE VIEW OF INTERFEROMETER TEST PLATE

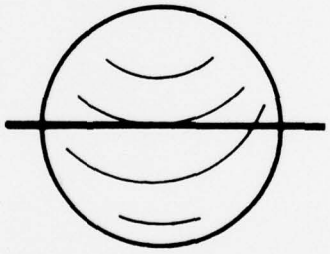

(b) TYPICAL FRINGE PATTERN OF UNCOLLIMATED BEAM

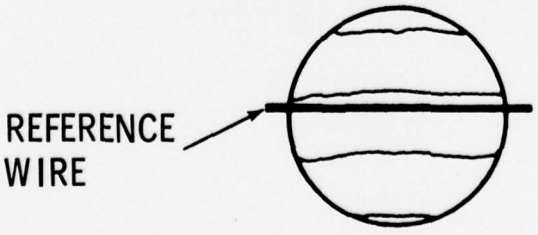

(c) FRINGE PATTERN OF COLLIMATED BEAM

Fig. 6 Plane wave interference in a shearing interferometer

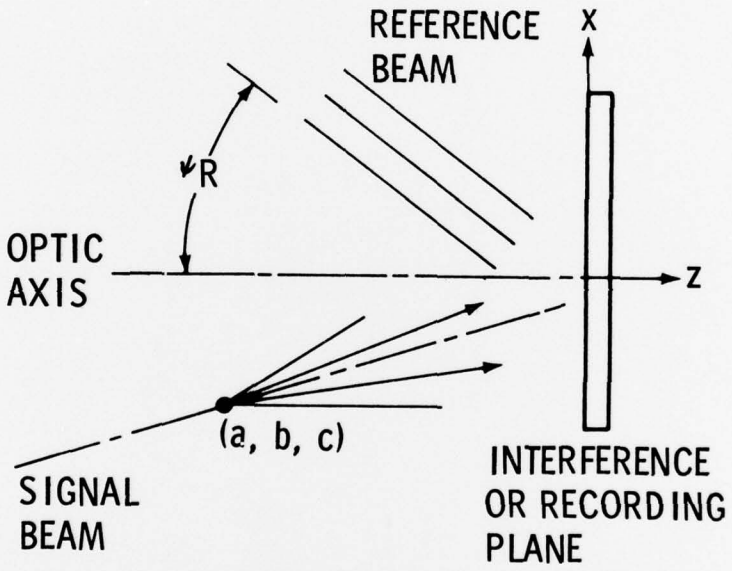

Fig. 7 Interference of plane and spherical waves

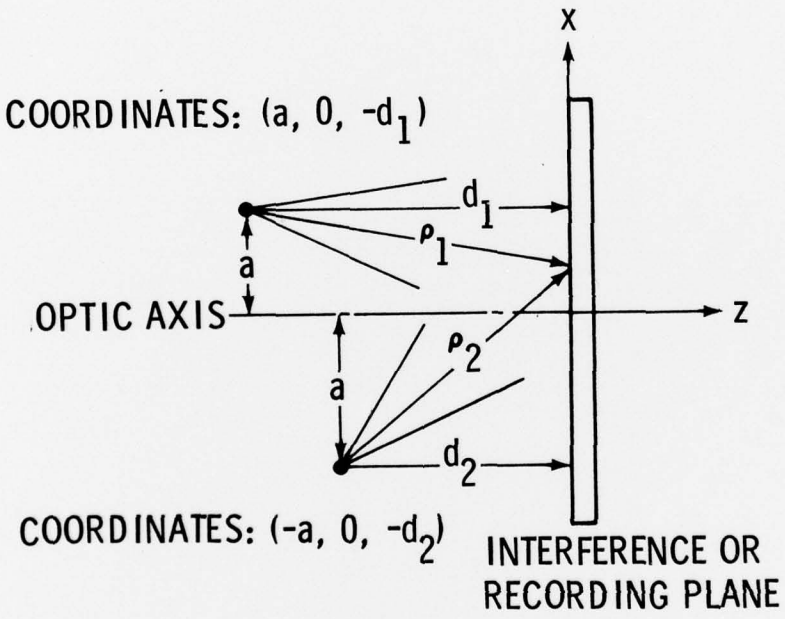

Fig. 8 Interference of two spherical waves